

Proton structure from a light-front Hamiltonian

Chandan Mondal,^{1,2,*} Siqi Xu,^{1,2,†} Jiangshan Lan,^{1,2,3,‡} Xingbo
Zhao,^{1,2,§} Yang Li,^{4,¶} Dipankar Chakrabarti,^{5,**} and James P. Vary^{4,††}

(BLFQ Collaboration)

¹*Institute of Modern Physics, Chinese Academy of Sciences, Lanzhou 730000, China*

²*School of Nuclear Science and Technology, University of Chinese Academy of Sciences, Beijing 100049, China*

³*Lanzhou University, Lanzhou 730000, China*

⁴*Department of Physics and Astronomy, Iowa State University, Ames, IA 50011, USA*

⁵*Department of Physics, Indian Institute of Technology Kanpur, Kanpur 208016, India*

We obtain the electromagnetic form factors, the axial form factor, and the parton distribution functions of the proton from the eigenstates of a light-front effective Hamiltonian in the leading Fock representation suitable for low-momentum scale applications. The electromagnetic and the axial form factors are found to be in agreement with the available experimental data. The unpolarized, the helicity, and the transversity valence quark distributions, after QCD evolution, are consistent with the global QCD analyses. The tensor charge also agree the experimental data, while the axial charge is somewhat outside the experimental error bar.

INTRODUCTION

Electromagnetic form factors (FFs) and parton distribution functions (PDFs) have taught us a great deal about the internal structure of the proton. The Fourier transform of these FFs provides information about spatial distributions of the proton's constituents [1, 2]. Well-known examples include the charge and magnetization distributions. Another essential tool to investigate hadron structure is deep inelastic scattering (DIS), where individual quarks are resolved. One can extract the PDFs from DIS, which encode the distribution of longitudinal momentum and polarization carried by the constituents. With an effective Hamiltonian for constituent quarks, suitable for low-resolution probes, we solve for the proton's light-front wavefunctions (LFWFs) used to produce the FFs and the PDFs. We compare our FFs with experimental data. We apply QCD evolution to our initial PDFs in order to incorporate degrees of freedom relevant to higher-resolution probes which allows us to compare our QCD-evolved PDFs with global fits to experimental data.

The matrix element of the electromagnetic current for the nucleon requires two independent FFs: the Dirac and Pauli FFs. We refer to Refs [3–7] for reviews of the experimental results and models on this subject. The nucleon electromagnetic FFs have been theoretically investigated in Refs. [8–27], while their flavor decomposition has been reported in Refs.[28–30]. Our work is motivated by the advent of high precision measurements of both proton and neutron FFs from ongoing and forthcoming experiments at Jefferson Lab [31–37].

PDFs reveal the internal structure of the nucleon in terms of number densities of confined quarks and gluons. At first approximation (“leading twist”), the spin structure of the nucleon is described in terms of three independent PDFs: the unpolarized $f_1(x)$, the helicity $g_1(x)$,

and the transversity $h_1(x)$, where x is the light-front longitudinal momentum fraction of the nucleon carried by quarks of flavor q . We provide these PDFs to assist in the analysis and interpretation of scattering experiments now and in the LHC era.

While the unpolarized and the helicity PDFs are fairly well determined [38–70], much less information is available on the transversity PDF. This distribution is important since it encodes the correlation between the transverse polarization of the constituents and the transverse polarization of the nucleon [71–80]. One of our aims is to predict the transversity PDF, compare with available data, and help motivate future challenging experiments.

Here, we adopt an effective light-front Hamiltonian between quarks and solve for its mass eigenstates at the scale suitable for low-resolution probes with the theoretical framework of basis light-front quantization (BLFQ) [81–84]. Our Hamiltonian includes the holographic QCD confinement potential [22] supplemented by the longitudinal confinement [84, 85] along with the one-gluon exchange (OGE) interaction [84] to account for the dynamical spin effects. By solving this Hamiltonian for the LFWFs in the constituent valence quark Fock space, and fitting the quark mass, confining strength, and coupling constants, we obtain good quality descriptions of its electromagnetic and axial FFs, radii, PDFs, axial and tensor charges.

PROTON WAVEFUNCTIONS FROM AN EFFECTIVE HAMILTONIAN

The structures of hadronic bound states are encoded in the LFWFs which are obtained as the eigenfunctions of the LF eigenvalue equation: $H_{\text{eff}}|\Psi\rangle = M^2|\Psi\rangle$, where H_{eff} is the effective Hamiltonian of the system with the mass squared (M^2) eigenvalue. In general, $|\Psi\rangle$ is the eigenvector in the Hilbert space spanned by all Fock sec-

tors. At the initial scale where the proton is described by three active quarks, we adopt the LF effective Hamiltonian H_{eff} defined by

$$H_{\text{eff}} = \sum_a \frac{\vec{p}_{\perp a}^2 + m_a^2}{x_a} + \frac{1}{2} \sum_{a \neq b} \kappa^4 \left[x_a x_b (\vec{r}_{\perp a} - \vec{r}_{\perp b})^2 - \frac{\partial_{x_a} (x_a x_b \partial_{x_b})}{(m_a + m_b)^2} \right] + \frac{1}{2} \sum_{a \neq b} \frac{C_F 4\pi \alpha_s}{Q_{ab}^2} \times \bar{u}_{s'_a}(k'_a) \gamma^\mu u_{s_a}(k_a) \bar{u}_{s'_b}(k'_b) \gamma^\nu u_{s_b}(k_b) g_{\mu\nu}, \quad (1)$$

where $\sum_a x_a = 1$, and $\sum_a \vec{p}_{\perp a} = 0$. $m_{a/b}$ is the mass of the quark, and κ is the strength of the confinement. x_a represents the LF momentum fraction carried by quark a . Meanwhile, \vec{p}_{\perp} is the relative transverse momentum, while $\vec{r}_{\perp} = \vec{r}_{\perp a} - \vec{r}_{\perp b}$, related to the holographic variable [22], is the transverse separation between two quarks. The last term in the effective Hamiltonian represents the OGE interaction where $Q_{ab}^2 = -q^2 = -(1/2)(k'_a - k_a)^2 - (1/2)(k'_b - k_b)^2$ is the average momentum transfer squared. $C_F = -2/3$ is the color factor, $g_{\mu\nu}$ is the metric tensor and α_s is the coupling constant. Here, $u_{s_a}(k_a)$ is the solution of the Dirac equation, with the subscript s_a representing spin and k_a is the momentum of quark a .

Following BLFQ, we expand $|\Psi\rangle$ in terms of the two dimensional harmonic oscillator ('2D-HO') basis in the transverse direction and the discretized plane-wave basis in the longitudinal direction [81, 82]. Each single-quark basis state is identified using four quantum numbers, $\bar{\alpha} = \{k, n, m, \lambda\}$. The longitudinal momentum of the particle is characterized by the quantum number k . The longitudinal coordinate x^- is confined to a box of length $2L$ with anti-periodic boundary conditions for fermions. As a result, the longitudinal momentum $p^+ = 2\pi k/L$ is discretized, where the dimensionless quantity $k = \frac{1}{2}, \frac{3}{2}, \frac{5}{2}, \dots$. All many-body basis states are selected to have the same total longitudinal momentum $P^+ = \sum_i p_i^+$, where the sum is over the quarks. We rescale P^+ using $K = \sum_i k_i$ such that $P^+ = \frac{2\pi}{L} K$. For a given quark i , the longitudinal momentum fraction x is defined as $x_i = p_i^+ / P^+ = k_i / K$.

The quantum numbers, n and m , denote radial excitation and angular momentum projection, respectively, of the particle within the 2D-HO basis, $\phi_{nm}(\vec{p}_{\perp})$ [81, 82]. The 2D-HO basis should form an efficient basis for systems subject to QCD confinement. For the quark spin, λ is used to label the helicity. Our multi-body basis states have fixed values of the total angular momentum projection $M_J = \sum_i (m_i + \lambda_i)$.

The valence wavefunction in momentum space is then

expanded as:

$$\Psi_{\{x_i, \vec{p}_{\perp i}, \lambda_i\}}^{M_J} = \sum_{\{n_i, m_i\}} \left\{ \psi(\{\bar{\alpha}_i\}) \prod_{i=1}^3 \frac{1}{b} \left(\frac{|\vec{p}_{\perp i}|}{b} \right)^{|m_i|} \sqrt{\frac{4\pi \times n_i!}{(n_i + |m_i|)!}} e^{im_i \theta_i} L_{n_i}^{|m_i|} \left(-\frac{\vec{p}_{\perp i}^2}{b^2} \right) \exp \left(-\frac{\vec{p}_{\perp i}^2}{2b^2} \right) \right\}, \quad (2)$$

where $\psi(\{\bar{\alpha}_i\})$ is the LFWF in the BLFQ basis obtained by diagonalizing Eq. (1) numerically. $b = 0.6$ GeV is the HO scale parameter and $\tan(\theta) = p_2/p_1$. Here $L_n^{|m|}$ is the associated Laguerre function. We truncate the infinite basis by introducing limit K_{max} such that, $\sum_i k_i = K_{\text{max}}$. In the transverse direction, we also truncate by limiting $N_{\alpha} = \sum_i (2n_i + |m_i| + 1)$ for multi-particle basis state to $N_{\alpha} \leq N_{\text{max}}$. The basis truncation corresponds to having a UV regulator $\Lambda_{\text{UV}} \sim b\sqrt{N_{\text{max}}}$. Since we are modeling the proton at a low-resolution scale, we select $N_{\text{max}} = 10$ and $K_{\text{max}} = 16.5$. To attempt to simulate the effect of higher Fock spaces and the other QCD interactions, we use a different quark mass in the kinetic energy, $m_{\text{q/KE}}$ and the OGE interaction, $m_{\text{q/OGE}}$. We set our parameters $\{m_{\text{q/KE}}, m_{\text{q/OGE}}, \kappa, \alpha_s\} = \{0.3 \text{ GeV}, 0.2 \text{ GeV}, 0.34 \text{ GeV}, 1.1\}$ to fit the proton mass and the flavor Dirac FFs [28–30]. For numerical convenience, we use a small gluon mass regulator ($\mu_g = 0.05$ GeV) in the OGE interaction. We find that our results are insensitive to $0.08 > \mu_g > 0.01$ GeV.

FORM FACTORS AND PDFS OF THE PROTON

In the LF formalism, the flavor Dirac $F_1^q(Q^2)$ and Pauli $F_2^q(Q^2)$ FFs in the proton can be expressed in terms of overlap integrals as [86]

$$F_1^q(Q^2) = \int_D \Psi_{\{x'_i, \vec{p}'_{\perp i}, \lambda_i\}}^{\uparrow*} \Psi_{\{x_i, \vec{p}_{\perp i}, \lambda_i\}}^{\uparrow},$$

$$F_2^q(Q^2) = -\frac{2M}{(q^1 - iq^2)} \int_D \Psi_{\{x'_i, \vec{p}'_{\perp i}, \lambda_i\}}^{\uparrow*} \Psi_{\{x_i, \vec{p}_{\perp i}, \lambda_i\}}^{\downarrow}, \quad (3)$$

with $\int_D \equiv \sum_{\lambda_i} \int \prod_i \left[\frac{dx d^2 \vec{p}_{\perp}}{16\pi^3} \right]_i 16\pi^3 \delta(1 - \sum x_j) \delta^2(\sum \vec{p}_{\perp j})$. For the struck quark of flavor q , $x'_1 = x_1$; $\vec{p}'_{\perp 1} = \vec{p}_{\perp 1} + (1 - x_1)\vec{q}_{\perp}$ and $x'_i = x_i$; $\vec{p}'_{\perp i} = \vec{p}_{\perp i} - x_i \vec{q}_{\perp}$ for the spectators ($i = 2, 3$). We consider the frame where the momentum transfer $q = (0, 0, \vec{q}_{\perp})$, thus $Q^2 = -q^2 = \vec{q}_{\perp}^2$.

Under charge and isospin symmetry, the proton FFs can be obtained from the flavor FFs [28]: $F_i^p = e_u F_i^u + e_d F_i^d$, where $e_u(e_d) = \frac{2}{3}(-\frac{1}{3})$, with the normalizations $F_1^u(0) = 2, F_2^u(0) = \kappa_u$ and $F_1^d(0) = 1, F_2^d(0) = \kappa_d$ where the anomalous magnetic moments for the up and the down quarks are $\kappa_u = 2\kappa_p + \kappa_n = 1.673$ and $\kappa_d = \kappa_p + 2\kappa_n = -2.033$. The nucleon Sachs FFs are

again written in terms of Dirac and Pauli FFs as

$$\begin{aligned} G_E^p(Q^2) &= F_1^p(Q^2) - \frac{Q^2}{4M_p^2} F_2^p(Q^2), \\ G_M^p(Q^2) &= F_1^p(Q^2) + F_2^p(Q^2), \end{aligned} \quad (4)$$

and the electromagnetic radii are defined by $\langle r_E^2 \rangle = -6 \frac{dG_E(Q^2)}{dQ^2} \Big|_{Q^2=0}$ and $\langle r_M^2 \rangle = -\frac{6}{G_M(0)} \frac{dG_M(Q^2)}{dQ^2} \Big|_{Q^2=0}$.

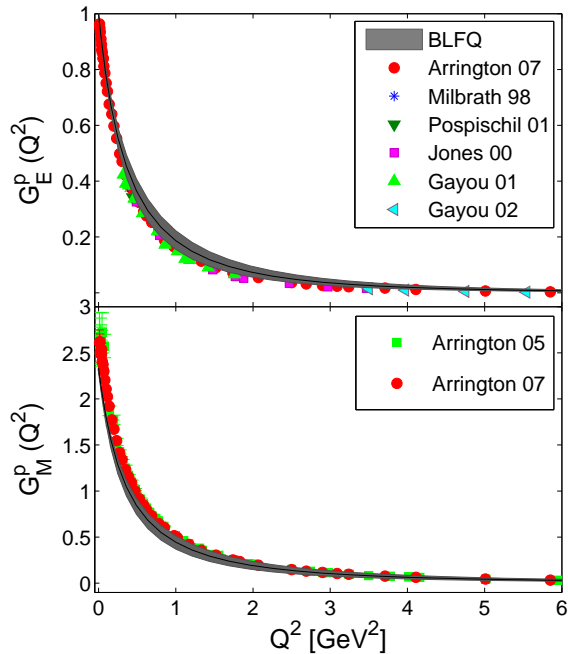


FIG. 1. Proton Sachs' FFs $G_E^p(Q^2)$ (upper panel), and $G_M^p(Q^2)$ (lower panel) as functions of Q^2 . The gray bands are BLFQ results reflecting our α_s uncertainty of 10%. The experimental data are taken from Refs.[87–92] and [89, 93].

In Fig. 1, we show the Q^2 dependence of the proton electric and the magnetic Sachs' FFs. Overall, we obtain a reasonable agreement between theory and experiment for the proton electric FFs. At large Q^2 , the magnetic form factor is also in good agreement with the data. However, our magnetic form factor at low Q^2 exhibits a small deviation from the data. It should be noted that the neglected higher Fock components $|qqq\bar{q}\bar{q}\rangle$ can have a significant effect on the magnetic form factor [17].

We present our computed radii in Table I and compare with measured data [94, 95] as well as with recent lattice QCD calculations [27]. Here again, we find reasonable agreement with experiment.

The axial form factor, which is identified with the matrix elements of axial-vector local operator, can also be expressed in terms of LFWFs

$$G_A^q(Q^2) = \int_D (\Lambda) \Psi_{\{x'_i, \vec{p}'_{\perp i}, \lambda_i\}}^{\uparrow*} \Psi_{\{x_i, \vec{p}_{\perp i}, \lambda_i\}}^{\uparrow}. \quad (5)$$

Here, $\Lambda = 1(-1)$ depends on the struck quark helicity $\lambda_1 = \frac{1}{2}(-\frac{1}{2})$. Experimental information about the axial

TABLE I. Proton radii, axial and tensor charges, first moments of transversity distributions. Our results are compared with the extracted data and recent lattice QCD calculations.

Quantity	BLFQ	Extracted data	Lattice
r_E fm	$0.802_{-0.040}^{+0.042}$	0.833 ± 0.010 [94]	$0.742(13)$ [27]
r_M fm	$0.834_{-0.029}^{+0.029}$	0.851 ± 0.026 [95]	$0.710(26)$ [27]
r_A fm	$0.680_{-0.073}^{+0.070}$	0.667 ± 0.12 [96]	$0.512(34)$ [97]
g_A	$1.41_{-0.06}^{+0.06}$	1.2723 ± 0.0023 [95]	$1.237(74)$ [97]
g_T^d	$-0.20_{-0.04}^{+0.02}$	$-0.25_{-0.10}^{+0.30}$ [73]	$-0.204(11)$ [98]
g_T^u	$0.94_{-0.15}^{+0.06}$	$0.39_{-0.12}^{+0.18}$ [73]	$0.784(28)$ [98]
$\langle x \rangle_T^{u-d}$	$0.229_{-0.048}^{+0.019}$	–	$0.203(24)$ [99]

FFs is very limited. Until now, there are only two sets of experiments: (anti)neutrino scattering off protons or nuclei and charged pion electroproduction [100, 101]. Fig. 2 shows the results obtained for the axial form factor, $G_A = G_A^u - G_A^d$ as a function of Q^2 , where we compare our BLFQ results with the experimental data [101, 102] and with lattice results [103]. Considering the theoretical and experimental uncertainties, the agreement is good. At $Q^2 = 0$, the axial form factor is the axial charge, $g_A = G_A(0)$. g_A is quoted in Table I, where we see our value differs somewhat from extracted data [95] and lattice [97]. We also evaluate the axial radius from: $\langle r_A^2 \rangle = \frac{6}{g_A} \frac{dG_A(Q^2)}{dQ^2} \Big|_{Q^2=0}$. As can be seen from the Table I, the BLFQ result is in good agreement with the extracted data from the analysis of neutrino-nucleon scattering experiment [96, 104].

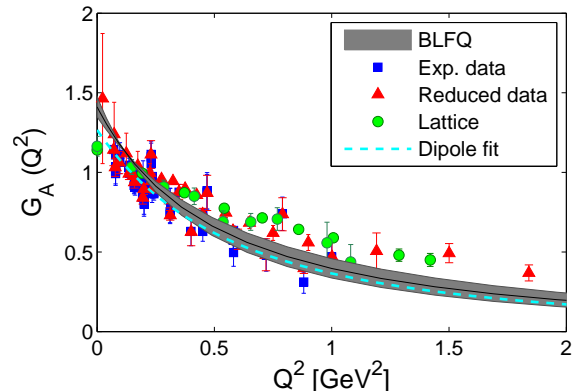


FIG. 2. Axial-vector form factor $G_A = G_A^u - G_A^d$ as function of Q^2 . The gray band is the BLFQ result. The extracted data are taken from the Refs. [101, 102] and the lattice data from [103]. The dashed line represents the dipole fit of the experimental data [101].

With our LFWFs, the proton's valence quark PDFs at

leading twist are given by

$$\begin{aligned}
 f_1^q &= \int_D \Psi_{\{x'_i, \vec{p}'_{\perp i}, \lambda_i\}}^{\uparrow*} \Psi_{\{x_i, \vec{p}_{\perp i}, \lambda_i\}}^{\uparrow} \delta(x - x_1), \\
 g_1^q &= \int_D (\Lambda) \Psi_{\{x'_i, \vec{p}'_{\perp i}, \lambda_i\}}^{\uparrow*} \Psi_{\{x_i, \vec{p}_{\perp i}, \lambda_i\}}^{\uparrow} \delta(x - x_1), \\
 h_1^q &= \int_D \left[\Psi_{\{x'_i, \vec{p}'_{\perp i}, \lambda_i\}}^{\uparrow*} \Psi_{\{x_i, \vec{p}_{\perp i}, \lambda_i\}}^{\downarrow} + (\uparrow \leftrightarrow \downarrow) \right] \delta(x - x_1),
 \end{aligned} \tag{6}$$

where the $\lambda'_1 = -\lambda_1$ and $\lambda'_{2,3} = \lambda_{2,3}$. At the model scale relevant to constituent quark masses which are several hundred MeV, the unpolarized PDFs for the valence quarks are normalized as $\int_0^1 f_1^u(x) dx = 2$, $\int_0^1 f_1^d(x) dx = 1$. We also have the following momentum sum rule: $\int_0^1 x f_1^u(x) dx + \int_0^1 x f_1^d(x) dx = 1$,

Next, to evolve our PDFs from our model scale, defined as μ_0^2 , to a higher scale μ^2 , we adopt the next-to-next-to-leading order (NNLO) Dokshitzer-Gribov-Lipatov-Altarelli-Parisi (DGLAP) equations [105–107] of QCD. This scale evolution allows quarks to emit and absorb gluons, with the emitted gluons capable of producing quark-antiquark pairs as well as additional gluons. In this picture, the sea quark and gluon components of the constituent quarks are revealed at the higher scale through QCD. While applying the DGLAP equations numerically [108], we impose the condition that the running coupling $\alpha_s(\mu^2)$ saturates in the infrared at a cutoff value of $\max \alpha_s = 1$ [109, 110], consistent with our fit value discussed above. We determine $\mu_0^2 = 0.195 \pm 0.020 \text{ GeV}^2$ by requiring the result after QCD evolution to produce the total first moments of the valence quark unpolarized PDFs from the global data fits with average values, $\langle x \rangle_{u_v+d_v} = 0.37 \pm 0.01$ at $\mu^2 = 10 \text{ GeV}^2$ [111].

Fig. 3 shows our results for the valence quark unpolarized and spin dependent PDFs of the proton, where we compare the valence quark distribution after QCD evolution with the global fits by MMHT14 [39], NNPDF3.0 [38] and CTEQ15 [40] Collaborations. The error bands in our evolved distributions are due to the spread in the initial scale $\mu_0^2 = 0.195 \pm 0.020 \text{ GeV}^2$ and the uncertainties in the coupling constant, $\alpha_s = 1.1 \pm 0.1$. Our unpolarized valence PDFs for both up and down quarks are found to be in good agreement with the global fits. Meanwhile, we evolve the spin dependent PDFs from our model scale to the relevant experimental scale $\mu^2 = 3 \text{ GeV}^2$ and find that the down quark helicity PDF agrees well with measured data from COMPASS Collaboration [51]. However, for the up quark, our helicity PDF tends to overestimate the data below $x \sim 0.3$.

The transversity distribution at $\mu^2 = 2.4 \text{ GeV}^2$ is also shown in Fig. 3. We compare our prediction with the global analysis of pion-pair production in DIS and in proton-proton collisions with a transversely polarized proton by Radici *et al.* [80], the global analysis of the data on azimuthal asymmetries in SIDIS, from the HERMES and COMPASS Collaborations, and e^+e^-

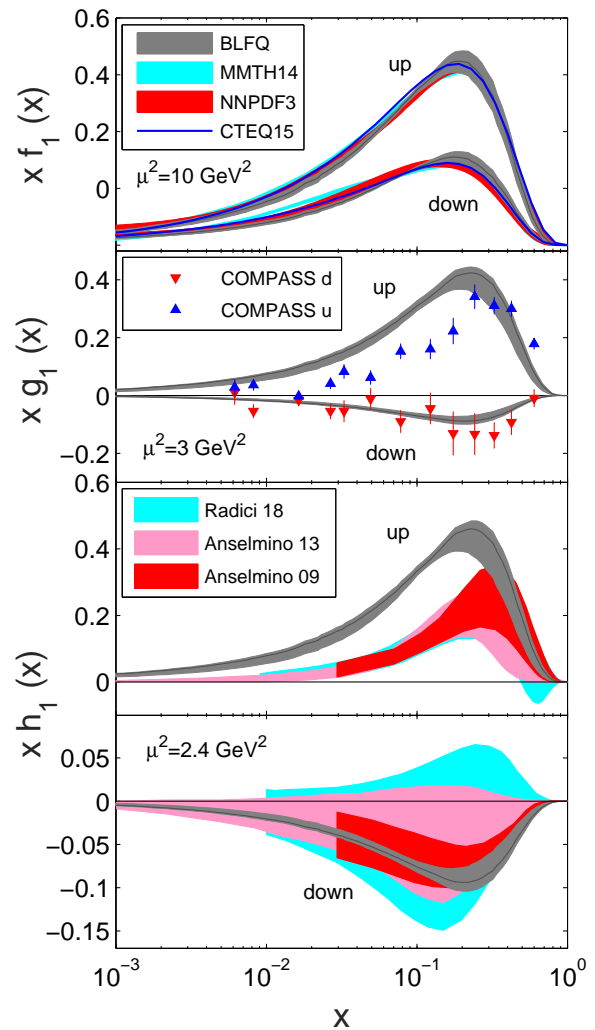


FIG. 3. Top panel: comparison for $x f_1(x)$ in the proton from BLFQ (gray bands) and global fits: MMHT14 [39] (cyan bands), NNPDF3.0 [38] (red bands), and CTEQ15 [40] (blue line). Second panel: comparison for $x g_1(x)$ in the proton from BLFQ (black bands) and measured data from COMPASS [51]. Lower two panel: Comparison for $x h_1(x)$ in the proton from BLFQ (gray bands) and global analyses by Radici *et al.* [80] (cyan bands) and Anselmino *et al.* [73] (pink bands), and [112] (red bands).

data from the BELLE Collaboration by Anselmino *et al.* [73, 112]. Our down quark transversity distribution is in accord with the fits. The up quark transversity distribution in our approach deviates in the low x region, while it shows reasonable agreement at large x with the global fits.

Transversity has recently received increasing attention because of the importance of a precise determination of its integral, the so-called tensor charge g_T . We compare our results at $\mu^2 = 2.4 \text{ GeV}^2$ with extracted data as well as with lattice data in Table I. Again we observe that BLFQ predicts the tensor charges quite well for down quark in comparison with the global QCD analysis [73]. However, for the up quark it deviates from the extracted

data but our value is closer to recent lattice data [98] and our approach yields comparable agreement with results from phenomenological models as well as other lattice calculations [113–116]. We also provide the first moments of transversity distribution, $\langle x \rangle_T^{u-d}$ in the Table I, which agree reasonably well with lattice data [99].

CONCLUSIONS

We present a model for the proton that provides observables from the low resolution constituent quark scale to high resolution experiments. Specifically, we begin with an effective LF Hamiltonian incorporating confinement and one gluon exchange interaction for the valence quarks suitable for low-resolution properties. Using basis LF quantization, the LFWFs obtained as the eigenvectors of this Hamiltonian were then used to generate the proton electromagnetic and axial form factors and the initial PDFs for different quark polarizations. We have obtained reasonable agreement with the experimental data for the Sach's FFs, the axial form factor as well as the electromagnetic radii for the proton. The unpolarized, helicity and transversity PDFs at higher scale relevant to global QCD analyses have been computed based on the NNLO DGLAP equations. The initial low-resolution scale is the only adjustable parameter involved in QCD scale evolution and we obtain it by fitting the first moments of unpolarized PDFs from global QCD analyses. We then find the unpolarized, the helicity, and transversity PDFs agree with results from the corresponding global fits or experimental data in Refs. [38–40], Ref. [51], and Refs. [80, 112], respectively. The axial charge and the tensor charge also show reasonable agreement with the extracted data or the lattice results. It should also be noted that basis truncation may play a role that should be examined in future research. The effective LFWFs can be used to study other parton distributions, such as the generalized parton distributions, the transverse momentum dependent parton distributions and the Wigner distributions. The presented results affirm the utility of our model and motivate application of analogous effective Hamiltonians to the other hadrons.

We thank Henry Lamm, Wei Zhu, Shuai Liu for many useful discussions. CM is supported by the National Natural Science Foundation of China (NSFC) under the Grant No. 11850410436. XZ is supported by new faculty startup funding by the Institute of Modern Physics, Chinese Academy of Sciences and by Key Research Program of Frontier Sciences, CAS, Grant No ZDBS-LY-7020. JPV is supported by the Department of Energy under Grants No. DE-FG02-87ER40371, and No. de-sc0018223 (SciDAC4/NUCLEI). A portion of the computational resources were provided by the National Energy Research Scientific Computing Center (NERSC), which is supported by the Office of Science of the U.S. Department

of Energy under Contract No. DE-AC02-05CH11231.

* mondal@impcas.ac.cn
† xsq123@impcas.ac.cn
‡ jiangshanlan@impcas.ac.cn
§ xzbzhao@impcas.ac.cn
¶ leeyoung@iastate.edu
** dipankar@iitk.ac.cn
†† jvary@iastate.edu

- [1] G. A. Miller, Phys. Rev. Lett. **99**, 112001 (2007).
- [2] C. E. Carlson and M. Vanderhaeghen, Phys. Rev. Lett. **100**, 032004 (2008).
- [3] H. Y. Gao, Int. J. Mod. Phys. E **12**, 1 (2003).
- [4] C. E. Hyde-Wright and K. de Jager, Ann. Rev. Nucl. Part. Sci. **54**, 217 (2004).
- [5] C. F. Perdrisat, V. Punjabi and M. Vanderhaeghen, Prog. Part. Nucl. Phys. **59**, 694 (2007).
- [6] S. Pacetti, R. Baldini Ferroli and E. Tomasi-Gustafsson, Phys. Rept. **550-551**, 1 (2015).
- [7] V. Punjabi, C. F. Perdrisat, M. K. Jones, E. J. Brash and C. E. Carlson, Eur. Phys. J. A **51**, 79 (2015).
- [8] C. Alexandrou, M. Constantinou, K. Hadjiyiannakou, K. Jansen, C. Kallidonis, G. Koutsou and A. Vaquero Aviles-Casco, Phys. Rev. D **96**, no. 3, 034503 (2017).
- [9] A. J. Chambers *et al.* [QCDSF and UKQCD and CSSM Collaborations], Phys. Rev. D **96**, no. 11, 114509 (2017).
- [10] E. Shintani, K. I. Ishikawa, Y. Kuramashi, S. Sasaki and T. Yamazaki, Phys. Rev. D **99**, no. 1, 014510 (2019).
- [11] F. He and P. Wang, Phys. Rev. D **97**, no. 3, 036007 (2018).
- [12] J. M. Alarcón and C. Weiss, Phys. Rev. C **97**, no. 5, 055203 (2018).
- [13] T. Gutsche, V. E. Lyubovitskij and I. Schmidt, Phys. Rev. D **97**, no. 5, 054011 (2018).
- [14] C. Mondal, Phys. Rev. D **94**, no. 7, 073001 (2016).
- [15] D. Chakrabarti and C. Mondal, Eur. Phys. J. C **73**, 2671 (2013).
- [16] D. Chakrabarti and C. Mondal, Phys. Rev. D **88**, no. 7, 073006 (2013).
- [17] R. S. Sufian, G. F. de Téramond, S. J. Brodsky, A. Deur and H. G. Dosch, Phys. Rev. D **95**, no. 1, 014011 (2017).
- [18] C. Mondal and D. Chakrabarti, Eur. Phys. J. C **75**, no. 6, 261 (2015).
- [19] T. Gutsche, V. E. Lyubovitskij, I. Schmidt and A. Vega, Phys. Rev. D **91**, 054028 (2015).
- [20] T. Gutsche, V. E. Lyubovitskij, I. Schmidt and A. Vega, Phys. Rev. D **89**, no. 5, 054033 (2014) Erratum: [Phys. Rev. D **92**, no. 1, 019902 (2015)].
- [21] C. Mondal and D. Chakrabarti, Few Body Syst. **57**, no. 8, 723 (2016).
- [22] S. J. Brodsky, G. F. de Téramond, H. G. Dosch and J. Erlich, Phys. Rept. **584**, 1 (2015).
- [23] Z. Ye, J. Arrington, R. J. Hill and G. Lee, Phys. Lett. B **777** (2018) 8.
- [24] Z. Abidin and C. E. Carlson, Phys. Rev. D **79**, 115003 (2009).
- [25] I. C. Cloet and G. A. Miller, Phys. Rev. C **86**, 015208 (2012).
- [26] B. Pasquini and S. Boffi, Phys. Rev. D **76**, 074011 (2007).

- [27] C. Alexandrou, S. Bacchio, M. Constantinou, J. Finkenrath, K. Hadjiyiannakou, K. Jansen, G. Koutsou and A. Vaquero Aviles-Casco, *Phys. Rev. D* **100**, no. 1, 014509 (2019).
- [28] G. D. Cates, C. W. de Jager, S. Riordan and B. Wojtsekhowski, *Phys. Rev. Lett.* **106**, 252003 (2011).
- [29] I. A. Qattan and J. Arrington, *Phys. Rev. C* **86**, 065210 (2012).
- [30] M. Diehl and P. Kroll, *Eur. Phys. J. C* **73**, no. 4, 2397 (2013).
- [31] JLab experiment E12-07-108, B. Wojtsekhowski, J. Arrington, S. Gilad and B. Moffit, spokespersons.
- [32] JLab experiment E12-07-109, B. Wojtsekhowski *et al.*, spokespersons.
- [33] JLab experiment E12-09-016, B. Wojtsekhowski, G. Cates and S. Riordan, spokespersons.
- [34] JLab experiment E12-09-019, B. Wojtsekhowski, J. Anand, R. Gilman and B. Quinn, spokespersons.
- [35] JLab experiment E12-07-104, W. Brooks, G. Gilfoyle, J. Lachniet, M. Vineyard, spokespersons.
- [36] JLab experiment E12-11-009, J. Arrington, K. Kohl, S. Kowalski, B. Sawatzky and A. Semenov, spokespersons.
- [37] JLab experiment E12-11-106, A. Gasparian, D. Dutta, H. Gao, M. Khandaker, spokespersons.
- [38] R. D. Ball *et al.* [NNPDF Collaboration], *Eur. Phys. J. C* **77**, no. 10, 663 (2017).
- [39] L. A. Harland-Lang, A. D. Martin, P. Motylinski and R. S. Thorne, *Eur. Phys. J. C* **75**, no. 5, 204 (2015).
- [40] S. Dulat *et al.*, *Phys. Rev. D* **93**, no. 3, 033006 (2016).
- [41] S. Alekhin, J. Blümlein, S. Moch and R. Placakyte, *Phys. Rev. D* **96**, no. 1, 014011 (2017).
- [42] A. D. Martin, W. J. Stirling, R. S. Thorne and G. Watt, *Eur. Phys. J. C* **63**, 189 (2009).
- [43] C. A. Aidala, S. D. Bass, D. Hasch and G. K. Mallot, *Rev. Mod. Phys.* **85**, 655 (2013).
- [44] A. Deur, S. J. Brodsky and G. F. De Tera mond, *Rept. Prog. Phys.* **82**, no. 076201 (2019).
- [45] X. Zheng *et al.* [Jefferson Lab Hall A Collaboration], *Phys. Rev. Lett.* **92**, 012004 (2004).
- [46] X. Zheng *et al.* [Jefferson Lab Hall A Collaboration], *Phys. Rev. C* **70**, 065207 (2004).
- [47] D. S. Parno *et al.* [Jefferson Lab Hall A Collaboration], *Phys. Lett. B* **744**, 309 (2015).
- [48] K. V. Dharmawardane *et al.* [CLAS Collaboration], *Phys. Lett. B* **641**, 11 (2006).
- [49] A. Airapetian *et al.* [HERMES Collaboration], *Phys. Rev. Lett.* **92**, 012005 (2004).
- [50] A. Airapetian *et al.* [HERMES Collaboration], *Phys. Rev. D* **71**, 012003 (2005).
- [51] M. G. Alekseev *et al.* [COMPASS Collaboration], *Phys. Lett. B* **693**, 227 (2010).
- [52] D. de Florian, R. Sassot, M. Stratmann and W. Vogelsang, *Phys. Rev. Lett.* **101**, 072001 (2008).
- [53] D. de Florian, R. Sassot, M. Stratmann and W. Vogelsang, *Phys. Rev. D* **80**, 034030 (2009).
- [54] E. R. Nocera *et al.* [NNPDF Collaboration], *Nucl. Phys. B* **887**, 276 (2014).
- [55] P. Jimenez-Delgado *et al.* [Jefferson Lab Angular Momentum (JAM) Collaboration], *Phys. Lett. B* **738**, 263 (2014).
- [56] J. J. Ethier, N. Sato and W. Melnitchouk, *Phys. Rev. Lett.* **119**, no. 13, 132001 (2017).
- [57] C. D. Roberts, R. J. Holt and S. M. Schmidt, *Phys. Lett. B* **727**, 249 (2013).
- [58] T. Liu, R. S. Sufian, G. F. de Téramond, H. G. Dosch, S. J. Brodsky and A. Deur, arXiv:1909.13818 [hep-ph].
- [59] K. F. Liu, *Phys. Rev. D* **62**, 074501 (2000).
- [60] K. F. Liu and S. J. Dong, *Phys. Rev. Lett.* **72**, 1790 (1994).
- [61] R. Horsley *et al.* [QCDSF and UKQCD Collaborations], *Phys. Lett. B* **714**, 312 (2012).
- [62] A. J. Chambers *et al.*, *Phys. Rev. Lett.* **118**, no. 24, 242001 (2017).
- [63] X. Ji, *Phys. Rev. Lett.* **110**, 262002 (2013).
- [64] H. W. Lin, J. W. Chen, S. D. Cohen and X. Ji, *Phys. Rev. D* **91**, 054510 (2015).
- [65] C. Alexandrou, K. Cichy, V. Drach, E. Garcia-Ramos, K. Hadjiyiannakou, K. Jansen, F. Steffens and C. Wiese, *Phys. Rev. D* **92**, 014502 (2015).
- [66] C. Alexandrou, K. Cichy, M. Constantinou, K. Hadjiyiannakou, K. Jansen, F. Steffens and C. Wiese, *Phys. Rev. D* **96**, no. 1, 014513 (2017).
- [67] A. V. Radyushkin, *Phys. Rev. D* **96**, no. 3, 034025 (2017).
- [68] K. Orginos, A. Radyushkin, J. Karpie and S. Zafeiropoulos, *Phys. Rev. D* **96**, no. 9, 094503 (2017).
- [69] Y. Q. Ma and J. W. Qiu, *Phys. Rev. Lett.* **120**, no. 2, 022003 (2018).
- [70] H. W. Lin *et al.*, *Prog. Part. Nucl. Phys.* **100**, 107 (2018).
- [71] R. L. Jaffe and X. D. Ji, *Phys. Rev. Lett.* **67**, 552 (1991).
- [72] M. Anselmino, M. Boglione, U. D'Alesio, A. Kotzinian, F. Murgia, A. Prokudin and S. Melis, *Nucl. Phys. Proc. Suppl.* **191**, 98 (2009).
- [73] M. Anselmino, M. Boglione, U. D'Alesio, S. Melis, F. Murgia and A. Prokudin, *Phys. Rev. D* **87**, 094019 (2013).
- [74] M. Anselmino, M. Boglione, U. D'Alesio, A. Kotzinian, F. Murgia, A. Prokudin and C. Turk, *Phys. Rev. D* **75**, 054032 (2007).
- [75] Z. B. Kang, A. Prokudin, P. Sun and F. Yuan, *Phys. Rev. D* **93**, no. 1, 014009 (2016).
- [76] M. Radici, A. Courtoy, A. Bacchetta and M. Guagnelli, *JHEP* **1505**, 123 (2015).
- [77] M. Radici, A. M. Ricci, A. Bacchetta and A. Mukherjee, *Phys. Rev. D* **94**, no. 3, 034012 (2016).
- [78] A. Bacchetta, A. Courtoy and M. Radici, *Phys. Rev. Lett.* **107**, 012001 (2011).
- [79] A. Bacchetta, A. Courtoy and M. Radici, *JHEP* **1303**, 119 (2013).
- [80] M. Radici and A. Bacchetta, *Phys. Rev. Lett.* **120**, no. 19, 192001 (2018).
- [81] J. P. Vary *et al.*, *Phys. Rev. C* **81**, 035205 (2010).
- [82] X. Zhao, H. Honkanen, P. Maris, J. P. Vary and S. J. Brodsky, *Phys. Lett. B* **737**, 65 (2014).
- [83] P. Wiecki, Y. Li, X. Zhao, P. Maris and J. P. Vary, *Phys. Rev. D* **91**, no. 10, 105009 (2015).
- [84] Y. Li, P. Maris, X. Zhao and J. P. Vary, *Phys. Lett. B* **758**, 118 (2016).
- [85] Y. Li, P. Maris and J. P. Vary, *Phys. Rev. D* **96**, no. 1, 016022 (2017).
- [86] S. J. Brodsky, M. Diehl, D. S. Hwang, *Nucl. Phys. B* **596**, 99 (2001).
- [87] O. Gayou *et al.*, *Phys. Rev. C* **64**, 038202 (2001).
- [88] O. Gayou *et al.*, *Phys. Rev. Lett.* **88**, 092301 (2002).

- [89] J. Arrington, W. Melnitchouk and J. A. Tjon, Phys. Rev. C **76**, 035205 (2007).
- [90] T. Pospischil *et al.*, Eur. Phys. J. A **12**, 125 (2001).
- [91] B. D. Milbrath *et al.*, Phys. Rev. Lett. **80**, 452 (1998).
- [92] M. K. Jones *et al.*, Phys. Rev. Lett. **84**, 1398 (2000).
- [93] J. Arrington, Phys. Rev. C **71**, 015202 (2005).
- [94] N. Bezhinov, T. Valdez, M. Horbatsch, A. Marsman, A. C. Vutha and E. A. Hessels, Science **365**, no. 6457, 1007 (2019).
- [95] M. Tanabashi *et al.* [Particle Data Group], Phys. Rev. D **98**, no. 3, 030001 (2018).
- [96] R. J. Hill, P. Kammel, W. J. Marciano and A. Sirlin, Rept. Prog. Phys. **81**, no. 9, 096301 (2018).
- [97] D. L. Yao, L. Alvarez-Ruso and M. J. Vicente-Vacas, Phys. Rev. D **96**, no. 11, 116022 (2017).
- [98] R. Gupta, B. Yoon, T. Bhattacharya, V. Cirigliano, Y. C. Jang and H. W. Lin, Phys. Rev. D **98**, no. 9, 091501 (2018).
- [99] C. Alexandrou *et al.*, arXiv:1908.10706 [hep-lat].
- [100] M. R. Schindler and S. Scherer, Eur. Phys. J. A **32**, no. 4, 429 (2007).
- [101] V. Bernard, L. Elouadrhiri and U. G. Meissner, J. Phys. G **28**, R1 (2002).
- [102] H. Hashamipour, M. Goharipour and S. S. Gousheh, Phys. Rev. D **100**, no. 1, 016001 (2019).
- [103] C. Alexandrou, M. Constantinou, S. Dinter, V. Drach, K. Jansen, C. Kallidonis and G. Koutsou, Phys. Rev. D **88**, no. 1, 014509 (2013).
- [104] A. S. Meyer, M. Betancourt, R. Gran and R. J. Hill, Phys. Rev. D **93**, no. 11, 113015 (2016).
- [105] Y. L. Dokshitzer, Sov. Phys. JETP **46**, 641 (1977) [Zh. Eksp. Teor. Fiz. **73**, 1216 (1977)].
- [106] V. N. Gribov and L. N. Lipatov, Sov. J. Nucl. Phys. **15**, 438 (1972) [Yad. Fiz. **15**, 781 (1972)].
- [107] G. Altarelli and G. Parisi, Nucl. Phys. B **126**, 298 (1977).
- [108] G. P. Salam and J. Rojo, Comput. Phys. Commun. **180**, 120 (2009); Higher Order Perturbative Parton Evolution toolkit.
- [109] J. Lan, C. Mondal, S. Jia, X. Zhao and J. P. Vary, Phys. Rev. Lett. **122**, no. 17, 172001 (2019).
- [110] J. Lan, C. Mondal, S. Jia, X. Zhao and J. P. Vary, arXiv:1907.01509 [nucl-th].
- [111] G. F. de Teramond *et al.* [HLFHS Collaboration], Phys. Rev. Lett. **120**, no. 18, 182001 (2018).
- [112] M. Anselmino, M. Boglione, U. D'Alesio, A. Kotzinian, F. Murgia, A. Prokudin and S. Melis, Nucl. Phys. Proc. Suppl. **191** (2009) 98 [arXiv:0812.4366 [hep-ph]].
- [113] M. Gockeler *et al.* [QCDSF and UKQCD Collaborations], Phys. Lett. B **627** (2005) 113 [hep-lat/0507001].
- [114] I. C. Cloet, W. Bentz and A. W. Thomas, Phys. Lett. B **659** (2008) 214 [arXiv:0708.3246 [hep-ph]].
- [115] B. Pasquini, M. Pincetti and S. Boffi, Phys. Rev. D **72** (2005) 094029 [hep-ph/0510376].
- [116] M. Wakamatsu, Phys. Lett. B **653** (2007) 398 [arXiv:0705.2917 [hep-ph]].